ELSEVIER

Materials Science and Engineering A309–310 (2001) 142–147

MATERIALS SCIENCE & ENGINEERING A

www.elsevier.com/locate/msea

Dislocation core properties of aluminum: a first-principles study

Gang Lu [a,*], Nicholas Kioussis [a], Vasily V. Bulatov [b], Efthimios Kaxiras [c]

[a] *Department of Physics, California State University Northridge, Northridge, CA 91330-8268, USA*
[b] *Lawrence Livermore National Laboratory, Livermore, CA 94550, USA*
[c] *Department of Physics, Harvard University, Cambridge, MA 02138, USA*

Abstract

We have employed the semidiscrete variational generalized Peierls–Nabarro model to study dislocation core properties of aluminum. The generalized stacking fault (GSF) energy surface entering the model is calculated by using first-principles density functional theory (DFT). Various core properties, including the core width, energetics and Peierls stress for different dislocations have been investigated. The correlation between the core energetics and the Peierls stress with the dislocation character has been explored. Our results reveal a simple relationship between the Peierls stress and the ratio between the core width and the atomic spacing.

Keywords: Dislocation cores; Stacking fault; Peierls stress

1. Introduction

There has been a great deal of interest in describing accurately the dislocation core structure on an atomic scale because of its important role played in many phenomena of crystal plasticity [1,2]. Two types of theoretical approaches have been employed to study the core properties of dislocations. The first type is based on direct atomistic simulations using either empirical potentials or first-principles calculations. Empirical interatomic potentials usually are not quite reliable in describing the finer dislocation core structures, where severe distortions like bond breaking, bond formation and switching necessitate a quantum mechanical description of the electronic degrees of freedom. On the other hand, first-principles electronic structure calculations, though considerably more accurate, are computationally expensive for the studies of dislocation properties. The second type, is based on the framework of the Peierls–Nabarro (P–N) model which seems to be a plausible alternative to direct atomistic simulations. In fact, there has been a resurgence of interest in the simple and tractable P–N model for the study of dislocation core structure and mobility [3–5]. In this paper we shall study the dislocation core properties of aluminum using the P–N model with the GSF energy surface obtained from first-principles calculations.

2. Computational method and the GSF energy surface

The GSF energy surface is calculated within the framework of density functional theory [6] (DFT) in the local density approximation [7] to the exchange-correlation functional, using the expression proposed by Perdew and Zunger [8]. A kinetic energy cutoff of 12 Ry for the plane wave basis is used and the atomic structures are considered fully relaxed when the Hellmann–Feynman forces on each atom are smaller than 0.001 Ry/au. The calculated equilibrium lattice constant and bulk modulus are 3.94 Å and 82.52 GPa, in good agreement with the corresponding experimental room-temperature values of 4.05 Å and 76.93 GPa, respectively.

In addition to the lattice constant and bulk modulus, we have calculated the value of the intrinsic stacking fault energy and the unstable stacking fault energy. The calculations are performed at the theoretically determined in-plane lattice constant. For the reciprocal space integration we have used a k-point grid consisting of (16, 16, 4) divisions along the reciprocal lattice directions according to the Monkhorst–Pack scheme [9]. Both atomic relaxations and volume relaxations were carried out to obtain accurate GSF energies. The value of the intrinsic stacking fault energy we obtained is 0.164 J/m^2, in excellent agreement with the result of 0.165 J/m^2 of Sun and Kaxiras [10] and that of 0.161 J/m^2 of Wright et al. [11]. Experimental measurements range from a low value of 0.110 J/m^2 to a high value of 0.280 J/m^2 [12]. Finally, the value of the relaxed unstable stacking fault energy is 0.224 J/m^2, in agreement with previous theoretical calculations [4,5].

* Corresponding author. Tel.: +1-818-677-2100; fax: +1-818-677-5615.
E-mail address: glu@newton.csun.edu (G. Lu).

0921-5093/01/$ – see front matter
PII: S0921-5093(00)01711-1

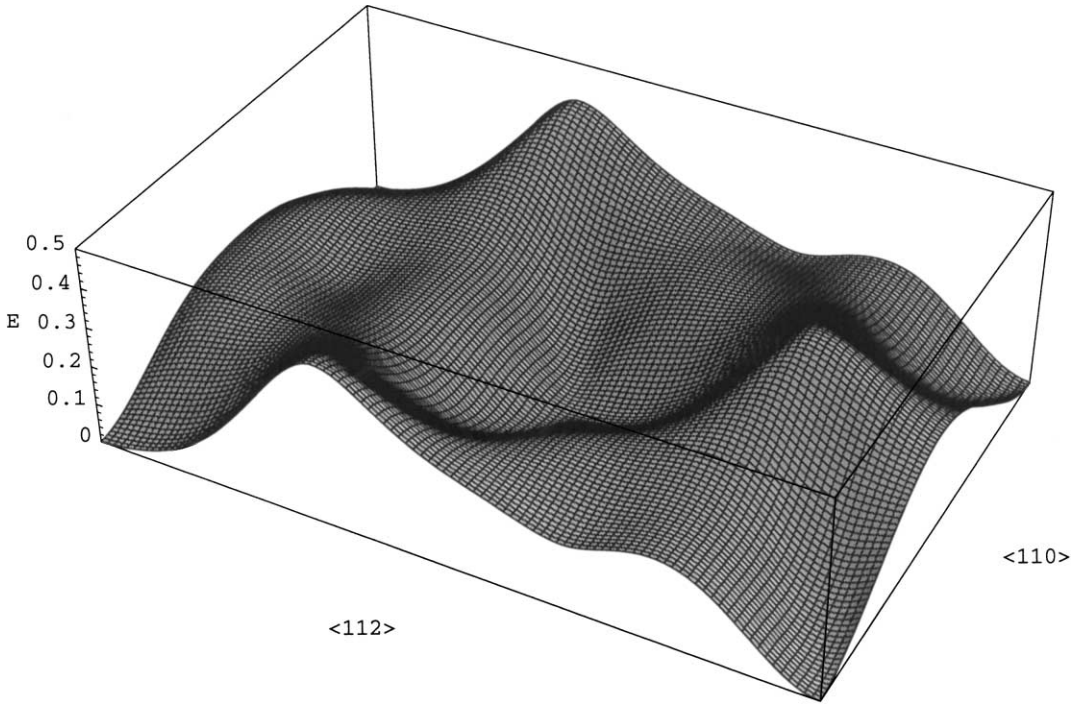

Fig. 1. The GSF energy surface for displacements along a (1 1 1) plane in Al (J/m^2) (the corners of the plane and its center correspond to identical equilibrium configurations, i.e. the ideal Al lattice) from DFT calculations.

The DFT GSF energy $\gamma(\vec{f})$ surface for the (1 1 1) plane is calculated on a grid of 40 points in the irreducible part of the (1 1 1) slip plane (1/12 of the area shown in Fig. 1). We use an augmented symmetrized polynomial basis to fit the calculated DFT GSF energy surface in order to facilitate the computation of dislocation properties. The basis is chosen so that it preserves the underlying translational and rotational symmetry of the fcc lattice. The fitted GSF energy surface is shown in Fig. 1, and the three high peaks of the GSF surface correspond to the run-on stacking fault configuration ABC|CABC, in which two C layers are the nearest neighbors. The local minimum and maximum along the $\langle 1\,1\,2\rangle$ direction correspond to the intrinsic and unstable stacking faults, respectively.

3. Semidiscrete variational P–N model

Recently a semidiscrete variational generalized P–N model has been proposed which appears to be a very promising approach to study dislocation core properties [13]. Within this approach, the equilibrium structure of a dislocation is obtained by minimizing the dislocation energy functional

$$U_{\text{disl}} = U_{\text{elastic}} + U_{\text{misfit}} + U_{\text{stress}} + Kb^2 \ln L, \tag{1}$$

where

$$U_{\text{elastic}} = \sum_{i,j} \tfrac{1}{2}\chi_{ij}[K_{\text{e}}(\rho_i^{(1)}\rho_j^{(1)} + \rho_i^{(2)}\rho_j^{(2)}) + K_{\text{s}}\rho_i^{(3)}\rho_j^{(3)}], \tag{2}$$

$$U_{\text{misfit}} = \sum_i \Delta x \gamma_3(\vec{f}_i), \tag{3}$$

$$U_{\text{stress}} = -\sum_{i,l} \frac{x_i^2 - x_{i-1}^2}{2}(\rho_i^{(l)}\tau_i^{(l)}), \tag{4}$$

with respect to the dislocation density or disregistry vector. Here, $\rho_i^{(1)}$, $\rho_i^{(2)}$ and $\rho_i^{(3)}$ are the edge, vertical and screw components of the general interplanar dislocation density at the i-th nodal point, and $\gamma_3(\vec{f}_i)$ is the three-dimensional misfit potential. The corresponding components of the applied stress interacting with the $\rho_i^{(1)}$, $\rho_i^{(2)}$ and $\rho_i^{(3)}$ are $\tau^{(1)} = \sigma_{21}$, $\tau^{(2)} = \sigma_{22}$ and $\tau^{(3)} = \sigma_{23}$, respectively. K is a constant depending on the elastic properties and the dislocation character and for an isotropic solid

$$K = \frac{\mu}{2\pi}\left(\frac{\sin^2\theta}{1-\nu} + \cos^2\theta\right). \tag{5}$$

The pre-logarithmic energy factors $K_{\text{e}} = \mu/(2\pi(1-\nu))$ and $K_{\text{s}} = \mu/2\pi$ are for an edge and a screw dislocation, respectively; $\mu = 28.8$ GPa and $\nu = 0.344$ are the shear modulus and Poisson's ratio for A1, respectively. The dislocation density at the i-th nodal point is $\rho_i^{(l)} = (f_i^{(l)} - f_{i-1}^{(l)})/(x_i - x_{i-1})$, $l = 1, 2, 3$, where $f_i^{(l)}$ and x_i are the three components of the disregistry vector and the coordinate of the i-th nodal point (atomic row), respectively. The x-axis is the dislocation gliding direction, which is always perpendicular to the dislocation line. The remaining quantities

entering in this expression are: $\chi_{ij} = 3/2\phi_{i,i-1}\phi_{j,j-1} + \psi_{i-1,j-1} + \psi_{i,j} - \psi_{i,j-1} - \psi_{j,i-1}$ with $\phi_{i,j} = x_i - x_j$ and $\psi_{i,j} = 1/2(\phi_{i,j}^2 \ln|\phi_{i,j}|)$. The quantity L entering the last term is the outer cutoff radius for the elastic energy [12].

The first term in the energy functional, U_{elastic}, represents the *configuration-dependent* (density or disregistry) part of the elastic energy, which has been discretized. This explicit discretization of the elastic energy term removes the inconsistency in the original P–N model and allows the total energy functional to be variational. Another improvement in this approach is that the nonlinear misfit potential in the energy functional, U_{misfit}, is a function of all three components of the nodal displacements, $\vec{f}(x_i)$. Namely, in addition to the displacements along the Burgers vector, lateral and even vertical displacements across the slip plane are also included. Furthermore, because the disregistry vector $\vec{f}(x_i)$ is allowed to change during the process of dislocation translation, the Peierls energy barrier can be significantly lowered compared

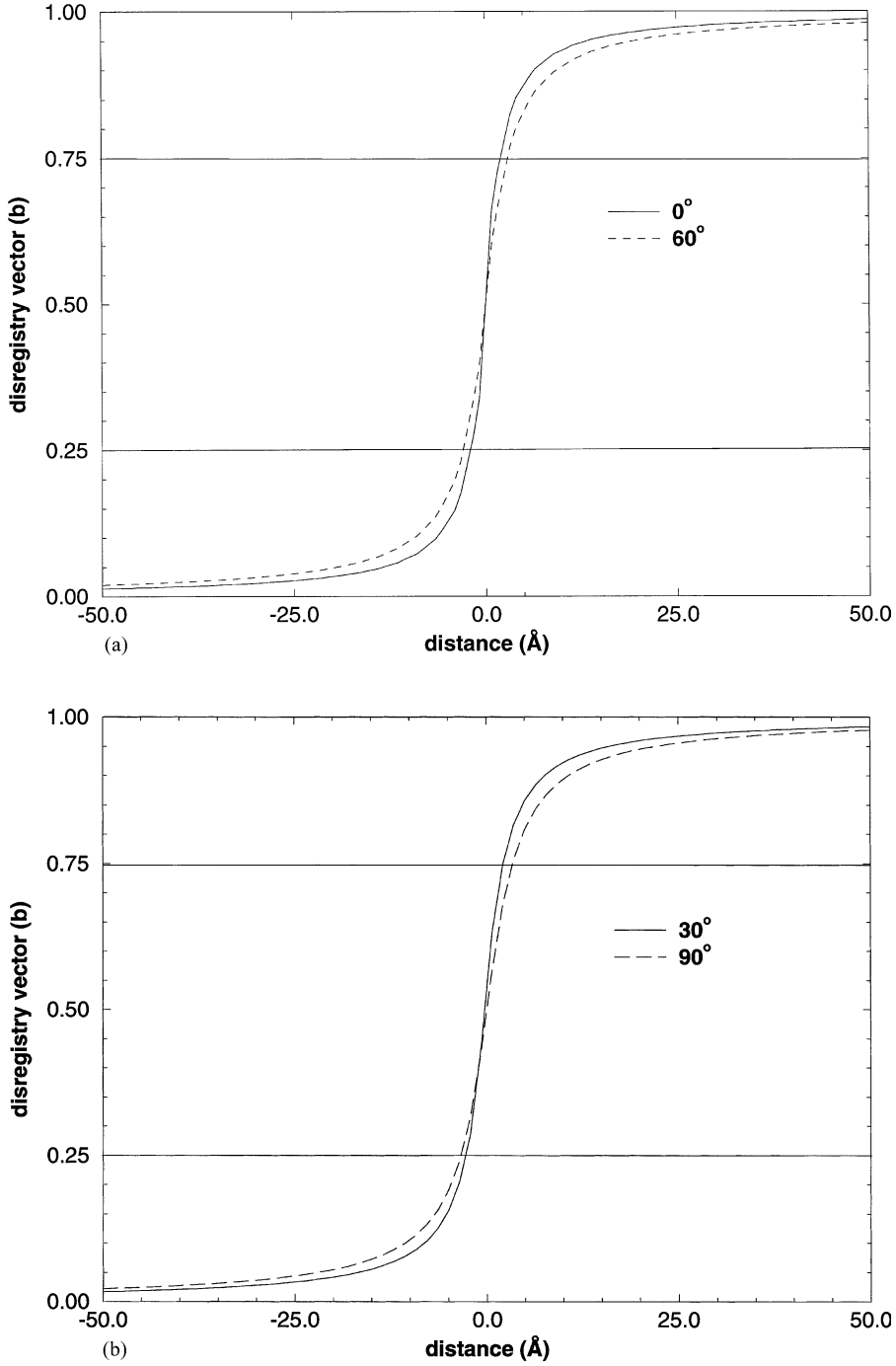

Fig. 2. The disregistry vector in units of the Burgers vector for: (a) the screw and 60° dislocations; (b) the 30° and edge dislocations.

to its corresponding value from a rigid translation. In order to examine the trend of energetics for different dislocations, we identify the dislocation *configuration-dependent* part of the total energy as the core energy, $U_{\text{core}} = U_{\text{elastic}} + U_{\text{misfit}}$, which includes the density-dependent part of the elastic energy and the entire misfit energy, in the absence of stress. The last term in Eq. (1), $Kb^2 \ln L$, is *independent* of the dislocation density, and hence it is irrelevant in the variational procedure. The outer cutoff radius L is chosen to be 10^3 Å for all dislocations.

The response of a dislocation to an applied stress is achieved by minimization of the energy functional with respect to ρ_i at the given value of the applied stress, $\tau_i^{(l)}$. An instability is reached when an optimal solution for ρ_i no longer exists, which is manifested numerically by the failure of the minimization procedure to convergence. The Peierls stress is defined as the critical value of the applied stress which gives rise to this instability.

4. Dislocation core properties

We first examine the core properties of four typical dislocations, i.e. the screw, 30°, 60° and edge dislocations. These dislocations have the same Burgers vector, $\vec{b} = a/2\ [1\,0\,1]$, but different orientations (characters). In order to examine the trend of the disregistry vector, $\vec{f} = f_1\hat{x} + f_2\hat{y} + f_3\hat{z}$, as a function of the angle θ between the dislocation line and the Burgers vector $\vec{b}$, one needs to determine the components of $\vec{f}$ parallel and perpendicular to b, i.e. $f_{\parallel} = f_1 \sin\theta + f_3 \cos\theta$ and $f_{\perp} = f_1 \cos\theta - f_3 \sin\theta$, respectively. The results for $f_{\parallel}$ are presented in Fig. 2(a) for the screw and 60° dislocations, and in Fig. 2(b) for the 30° and edge dislocations, respectively.

The dislocation half width ζ, defined as the atomic distance over which $f_{\parallel}$ changes from $1/4b$ to $3/4b$ can be determined from Fig. 2. The values of ζ for the four dislocations are listed in Table 1 and one can see the trend that the half width increases monotonically with the dislocation angle θ.

The results for the energetics and the Peierls stress for the four dislocations are also presented in Table 1. The misfit energy, U_{misfit}, increases monotonically from the screw to the edge dislocation, while the *configuration-dependent* elastic energy, U_{elastic} (negative in sign) decreases as the angle increases. The *configuration-independent* elastic energy $Kb^2 \ln L$ is also included. Several points need to be emphasized: (1) The *configuration-dependent* elastic energy U_{elastic}, ignored in some previous studies, is the dominant contribution to the core energy U_{core} (about a factor of two larger than U_{misfit}). More importantly, it depends strongly on the dislocation character; (2) While U_{elastic} is negative here, in principle, it can be of either sign. For example, U_{elastic} was found to be positive in Si [15]; (3) Inclusion of the *configuration-independent* elastic term, $Kb^2 \ln L$, yields positive values for both the total energy and the total elastic energy.

Table 1
Core half widths ζ (in Å); core energies U_{core} and separate contributions from the *configuration-dependent* elastic energy, U_{elastic} and the misfit energy U_{misfit}; $Kb^2 \ln L$ (in eV/Å); and Peierls stress (in MPa) for the four dislocations

	Screw	30°	60°	Edge
Core widths	2.1	2.5	3.0	3.5
U_{core}	−0.0834	−0.1096	−0.1678	−0.1979
U_{elastic}	−0.1828	−0.2317	−0.3199	−0.3666
U_{misfit}	0.0938	0.1221	0.1521	0.1688
$Kb^2 \ln L$	1.6050	1.8123	2.233	2.446
Peierls stress	256	53	98	35

As alluded earlier, the Peierls stress in this work is calculated as the critical value of the applied stress τ, at which the dislocation energy functional fails to be minimized with respect to ρ_i through standard conjugate gradient techniques. This approach is more accurate and physically transparent, because it captures the nature of the Peierls stress as the stress at which the displacement field of the dislocation undergoes a discontinuous transition. A typical value for the Peierls stress of Al from the analysis of the Bordoni internal peaks is about 230 MPa [14] which is very close to our value for the screw dislocation.

5. Correlation between dislocation properties and dislocation character

In an effort to correlate dislocation properties with the dislocation character, we have studied the dislocation properties of 19 different dislocations that have the same Burgers vector but different orientations. The angle between the dislocation line and the Burgers vector varies from 0 to 90°.

The core energy U_{core} along with its separate contributions from the *configuration-dependent* elastic energy U_{elastic} and the misfit energy U_{misfit}, are presented in Fig. 3 as a function of the dislocation angle θ. We find that and U_{elastic} decrease monotonically as the angle increases, whereas U_{misfit} increases with θ. The *configuration-dependent* elastic energy U_{elastic} decreases with θ because the pre-logarithmic factor K increases with θ. On the other hand, the monotonic increase of U_{misfit} with θ is due to the fact that the core width increases with the dislocation angle. Note, that the *configuration-dependent* elastic energy, not only is the dominant contribution to the total energy stored in the core region, but also is more sensitive to the dislocation character than the misfit energy.

In order to correlate the Peierls stress with the dislocation character, plotted in Fig. 4 is $\ln(\sigma_p \bar{a}/Kb)$ as a function of $\zeta/\bar{a}$. Here, ζ is the half width of a dislocation and $\bar{a}$ is the average nodal spacing along the X direction. It should be pointed out that most of the dislocations in the fcc lattice have non-even nodal spacings, except for the 30° and edge dislocations. Most of the calculated values can be fitted

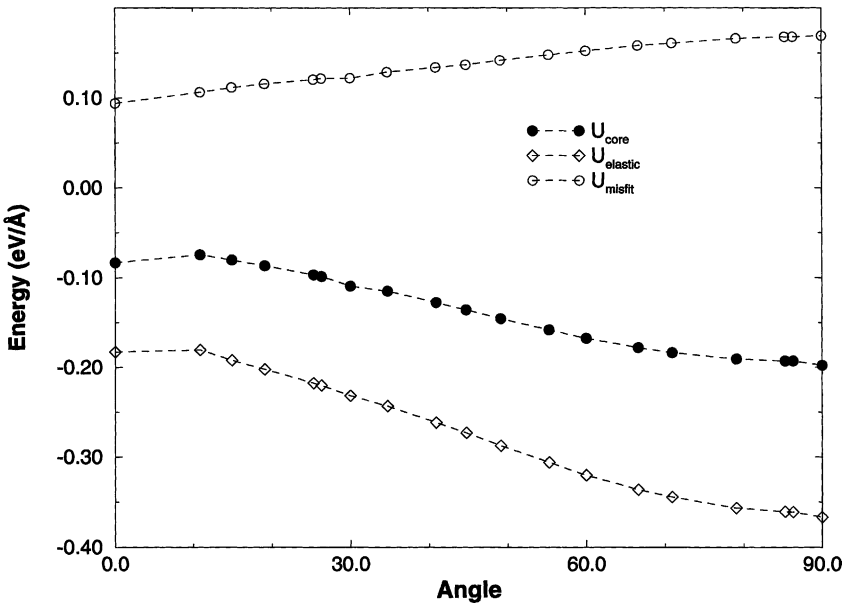

Fig. 3. The core energy, elastic energy and misfit energy as a function of dislocation orientations.

(solid line) with

$$\sigma_{\mathrm{p}} = \frac{2\pi K b}{\bar{a}} \mathrm{e}^{-1.7\zeta/\bar{a}}. \tag{6}$$

The large deviation of σ_{p} for the 30° and edge dislocations from the common trend, indicates that the nodal spacing (even versus non-even) between atomic planes plays an important role on the Peierls stress [15]. On the other hand, the deviation of the 10.9 and 14.9° dislocations from the common trend is unclear at present. Note, that the Peierls stress is more sensitive to the average atomic spacing $\bar{a}$ than to the half width. For example, while both the 0 and 14.9° dislocations have predominant screw components and similar half widths of 2.1 and 2.3 Å, respectively, they have quite different atomic spacings, 1.2 and 0.3 Å, respectively. This results in a Peierls stress of 6 MPa for the 14.9° dislocation, almost two orders of magnitude smaller than that of 256 MPa for the screw dislocation.

In conclusion, we have performed first-principles calculations to obtain the GSF energy surface for the (1 1 1) glide plane of Al. From these calculations we extracted the core properties for various dislocations, using the semidiscrete

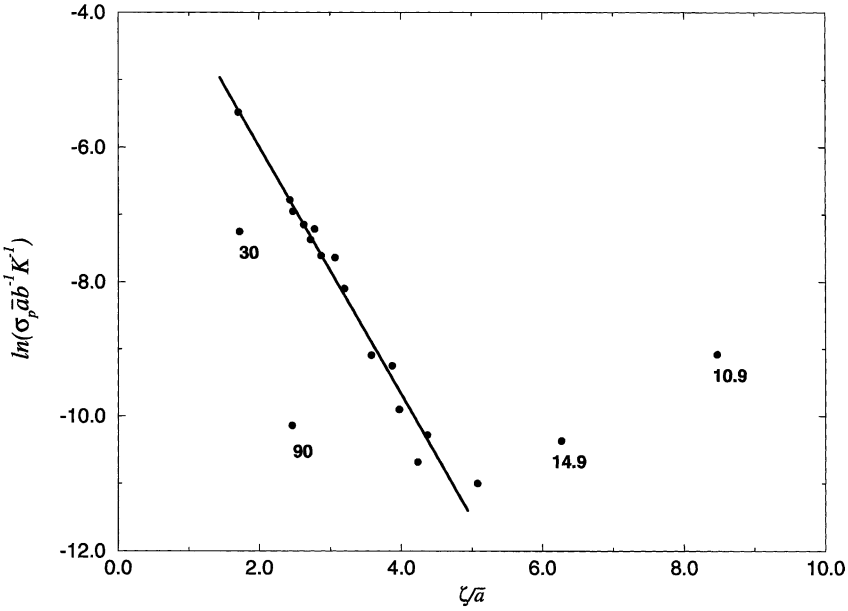

Fig. 4. The scaled Peierls stress as a function of the ratio of the core width to the average atomic spacing perpendicular to the dislocation line.

variational generalization of the P–N model. We have shown that the accurate DFT calculations of the GSF surface combined with the semidiscrete variational P–N model enable us to study the dislocation core properties more accurately and expediently. Moreover, this model can be extended to study a wide range of problems that are associated with more complex dislocations processes such as cross slip, dislocation intersections, reactions, etc.

Acknowledgements

The work at California State University Northridge was supported by the Grant no. DAAG55-97-l-0093 through the US Army Research Office. The work of EK is supported by the Harvard Materials Research Science and Engineering Center, which is funded by NSF Grant no. DMR-94-00396.

References

[1] M.S. Duesbery, G.Y. Richardson, CRC Crit. Rev. Solid State Mater. Sci. 17 (1991) 1.
[2] V. Vitek, Prog. Mater. Sci. 36 (1992) 1.
[3] B. Joós, Q. Ren, M.S. Duesbery, Phys. Rev. B 50 (1994) 5890.
[4] Y. Juan, E. Kaxiras, Philos. Mag. A 74 (1996) 1367.
[5] J. Hartford, B. von Sydow, G. Wahnström, B.I. Lundqvist, Phys. Rev. B 58 (1998) 2487.
[6] P. Hohenberg, W. Kohn, Phys. Rev. 136 (1964) B864.
[7] W. Kohn, L. Sham, Phys. Rev. 140 (1965) A1133.
[8] J. Perdew, A. Zunger, Phys. Rev. B. 23 (1984) 5048.
[9] H.J. Monkhorst, J.D. Pack, Phys. Rev. B 13 (1976) 5188.
[10] Y. Sun, E. Kaxiras, Philos. Mag. A 75 (1997) 1117.
[11] A. Wright, M.S. Daw, C.Y. Fong, Philos. Mag. A 66 (1992) 387.
[12] J.P. Hirth, J. Lothe, Theory of Dislocations, 2nd Edition, Wiley, New York, 1992.
[13] V.V. Bulatov, E. Kaxiras, Phys. Rev. Lett. 78 (1997) 4221.
[14] F.R.N. Nabarro, Philos. Mag. A 75 (1997) 703.
[15] G. Lu, N. Kioussis, V. Bulatov, E. Kaxiras, Philos. Mag. Lett. 80 (2000) 675.